Inner-shell photoionization of ground-state lithium: Theoretical calculation in the photon energy region of hollow atomic states

L. Vo Ky,[1] P. Faucher,[1] H. L. Zhou,[2] A. Hibbert,[3] Y.-Z. Qu,[4] J.-M. Li,[4] and F. Bely-Dubau[1]
[1]*UMR du CNRS 6529, Observatoire de la Côte d'Azur, Boîte Postale 4229, 06304 Nice Cedex, France*
[2]*Department of Physics and Astronomy, Georgia State University, Atlanta, Georgia 30303-3083*
[3]*Queen's University of Belfast, BT7 1NN Belfast, United Kingdom*
[4]*Institute of Physics, Chinese Academy of Science, Beijing 100080, China*
(Received 6 November 1996; revised manuscript received 27 April 1998)

Photoion and photoelectron data for hollow lithium states were recently reported with increased spectral resolution. In order to reproduce and identify the important resonances due to $2ln'l'n''l''\ ^2P^o$ autoionizing states new photoionization calculations have been performed using the *R*-matrix code with a 29-term target representation for incident photon energies between 140 and 167 eV. Excellent agreement between theoretical and measured results over partial or total photoionization cross sections confirms the quality of the theoretical model. A determination of the resonance positions for each series converging to a $2l2l'\ ^{1,3}L$ threshold of Li is proposed. [S1050-2947(98)04411-4]

PACS number(s): 32.80.Fb, 32.80.Hd

I. INTRODUCTION

The photoexcitation and decay dynamics of hollow Li atoms in which both *K*-shell electrons are excited have been the subject of intense recent experimental and theoretical interest. The first observation of a photon-induced triply excited state was performed by Kiernan *et al.* [1] using the dual laser plasma technique. These authors measured the position, width, and profile index of the $1s^22s\ ^2S-2s^22p\ ^2P^o$ transition in the photoabsorption spectrum, at a photon energy of around 142.3 eV. A much wider energy range (140–165 eV) was studied by the same team (Kiernan *et al.* [2]). A number of higher resonances were found and tentatively classified by means of configuration interaction calculations using the Cowan code [3]. Further experiments in this energy range by Azuma *et al.* [4] revealed yet more resonances, which were again identified by theoretical analysis, in this case using the multiconfigurational Dirac-Fock process.

The first measurements of partial cross sections were made by Journel *et al.* [5], and very recently this work was extended by Diehl *et al.* [6–8] with much greater resolution and over a wider energy range. These papers also describe preliminary calculations of these cross sections using the *R*-matrix method.

A number of other theoretical methods have been used to study triply excited states of Li. Early calculations include determinations of the photoionization width of the $2s^22p\ ^2P^o$ resonance using a Z^{-1} expansion method [9] and many-body perturbation theory (MBPT) [10]. The positions of a number of resonances in Li and in some Li-like ions were calculated by Piangos and Nicolaides [11] by the multiconfigurational Hartree-Fock method. More recently, the positions and widths of these resonances were determined using the saddle-point complex-rotation method by Chung and Gou [12,13]. Their calculations are the most extensive to date and include a careful analysis of relativistic corrections.

However, the only calculations of photoionization cross sections that have been published to date are those described in [5–8]. We now wish to describe those calculations in much greater detail. In a first paper [14], hereafter referred to as paper I, the process of inner-shell photoionization of the ground state of the Li atom was studied in the photon energy region below 130 eV including $1snln'l'$ Rydberg series of resonances. In this *R*-matrix calculation, the close coupling (CC) expansion of the Li^+ target was represented by 19 states of the form $1snl$ ($n\leqslant 4$) and the configuration interaction (CI) expansion of those states included up to 103 basic configurations, allowing for electron correlation effects. In the present study, covering the photon energy range 140–167 eV, in which lie the $2l2l'n''l''$ resonant states, the target state representation must be extended to include doubly excited Li^+ states. In Sec. II, we describe how these target states were determined. In Sec. III, we detail the *R*-matrix calculations using those target states. Then in Secs. IV–VII we present results of total and partial photoionization cross sections, branching ratios, asymmetry parameters (β), and energy positions of the resonances.

II. TARGET STATE CALCULATIONS

The partial and total cross sections, as well as the β asymmetry parameters, have been calculated using the *R*-matrix method as described in paper I. The wave function for the target+electron system, with total symmetry $SL\pi$ is given by

$$\Psi^{SL\pi}=A\sum_{i=1}^{N^F} c_i\phi_i(S_iL_i;\mathbf{x}_1,\ldots,\mathbf{x}_N,\hat{\mathbf{x}}_{N+1})F(k_il_i;r_{N+1})r_{N+1}^{-1}+\sum_{j=1}^{N^B} d_j\Phi_j^{SL\pi}, \quad (1)$$

where the different notations are defined in paper I. The $(N+1)$-electron functions $\Phi_j^{SL\pi}$ are configuration state functions built entirely from the bound orbitals. The functions ϕ_i are built by coupling the angular and spin functions of the

additional electron with the wave functions $\Phi_i(S_iL_i)$ of the target terms that are included in the close-coupling (CC) expansion. In this section we discuss the calculation of these target state functions $\Phi_i(S_iL_i)$. They are represented by CI expansions of the form

$$\Phi_i(S_iL_i)=\sum_{j=1}^{M} a_j\psi_j(S_iL_i), \tag{2}$$

where the configuration state functions (CSFs) ψ_i are constructed from one-electron orbitals of the form

$$\frac{1}{r}P_{nl}(r)Y_l^{m_l}(\theta,\phi)\chi_{m_s}(\sigma) \tag{3}$$

with the angular momenta coupled to form a total S_iL_i. The coefficients $\{a_i\}$ are the eigenvector components of the Hamiltonian matrix whose typical element is $\langle\psi_j|H_N|\psi_k\rangle$ where H_N is the N-electron Hamiltonian. The corresponding eigenvalues E_k of any $S_iL_i\pi$ symmetry are the calculated target state energies, and satisfy the inequalities

$$E_k \geqslant E_k^{\text{exact}}, \tag{4}$$

where we assume the eigenvalues are ordered: $E_1<E_2<E_3<\cdots$.

The inequalities (4) constitute variational principles from which to optimize the radial functions $P_{nl}(r)$ in Eq. (3). They apply equally to the ground and excited bound states [15] as to doubly excited states of two-electron ions [16]. Specifically, each radial function may be optimized by minimizing one (or a linear combination) of the $\{E_k\}$, potentially a different eigenvalue for each radial function.

The target states in these calculations have been determined using the code CIV3 [17], in which the radial functions $P_{nl}(r)$ are expressed in analytic form:

$$P_{nl}(r)=\sum_{j=1}^{k} c_{jnl}r^{I_{jnl}}\exp(-\zeta_{jnl}r). \tag{5}$$

TABLE I. Method of optimization.

Orbital	Energy functional optimized
$\overline{5s},\overline{5p}$	$2s^2\ {}^1S$, with all configurations *msns*; $m,n\leqslant 5$ and $2p^2$, $2p3p$, $2p4p$, $2p\overline{5p}$.
$\overline{5d}$	$2p^2\ {}^1D$, with all configurations *msnd*; $m,n\leqslant 5$ and $2p^2$, $2p3p$, $2p4p$, $2p\overline{5p}$, $3p^2$
$\overline{6s},\overline{6p}$	$1s^2\ {}^1S$ with configurations $1s^2$, $1s2s$, $1s\overline{5s}$, $1s\overline{6s}$, $2s^2$, $2s3s$, $2s4s$, $2s\overline{5s}$, $2s\overline{6s}$, $3s^2$, $3s4s$, $3s\overline{5s}$, $4s\overline{5s}$, $\overline{6s^2}$, $2p^2$, $2p3p$, $2p4p$, $3p4p$, $2p\overline{5p}$, $2p\overline{6p}$
$\overline{6d}$	$1s^2\ {}^1S$ with configurations $1s^2$; *mdnd*, $m,n\leqslant 6$

In paper I, we optimized the functions of $1s\cdots4f$ to give ''spectroscopic'' orbitals describing the target states of the form $1snl(n\leqslant 4)$, with three further correlation orbitals optimized on the $1s^2\ {}^1S$ ground-state energy. In this paper, we retain these $1s\cdots4f$ orbitals, but we have extended the correlation orbital set: $\overline{5s}$, $\overline{5p}$, $\overline{5d}$ are optimized on the doubly excited Li^+ states, while $6s$, $6p$, $6d$ are optimized on the $1s^2\ {}^1S$ ground-state energy. Specific details of the optimization process are presented in Table I while the radial function parameters [of Eq. (5)] of these correlation functions are given in Table II. (The parameters for $1s\cdots4f$ were given in paper I.)

The 19 target states used in paper I—those of the form $1snl$—are here augmented by 10 doubly excited target states: 6 states from $2s^2$, $2s2p$, $2p^2$ and 4 from $2s3s$ and the lowest ${}^1P^o$, ${}^3P^o$ combinations of $2s3p$ and $2p3s$ (sometimes written as $23sp$ because of the strong CI mixing between them). The CI expansions (2) include a total of 151 ''basic'' configurations, giving a total of 369 configuration couplings for the 29 target states.

The calculated target state energies are shown in Table III, where we compare our values with experiment and the previous calculations of paper I. The difference between the calculated and experimental separations is almost constant—approximately 1500 cm^{-1} or 0.2 eV, indicating that it is the

TABLE II. Radial function parameters for correlation orbitals of the Li^+ target.

Orbital (nl)	C_{jnl}	I_{jnl}	ζ_{jnl}	Orbital (nl)	C_{jnl}	I_{jnl}	ζ_{jnl}
$\overline{5s}$	5.31168	1	0.73299	$\overline{6p}$	2.65518	2	2.31445
	−4.68498	2	1.63529		−3.17379	3	2.22769
	−0.48025	3	1.72505		1.25699	4	1.43230
	−2.19063	4	0.67873		−1.27705	5	0.66613
	1.18295	5	0.57645		1.00689	6	0.62751
$\overline{6s}$	5.74190	1	1.04567	$\overline{5d}$	1.36803	3	1.35375
	−15.77683	2	1.27744		−1.11928	4	0.90556
	−1.41093	3	0.44009		0.42336	5	0.49091
	6.79730	4	1.81189	$\overline{6d}$	1.02379	3	6.14002
	4.30001	5	3.19898		−0.21190	4	0.90556
	1.70750	6	0.88228		0.15327	5	0.74705
$\overline{5p}$	1.22290	2	1.75061		−0.12398	6	0.63131
	−1.99255	3	0.96964				
	2.89668	4	0.63272				
	−1.87869	5	0.58887				

TABLE III. Target state energies relative to the $1s^2\ ^1S$ ground state of Li^+ ($E=-7.27264$ a.u.).

	Energies			
	This work		Experimental[b]	Paper I
State	(a.u.)	(cm^{-1} or eV)[a]	(cm^{-1} or eV)[a]	(cm^{-1})
$1s^2\ ^1S$	0	0	0	0
$1s2s\ ^3S$	2.16229	474567	476046	474965
$1s2s\ ^1S$	2.23316	490122	491361	489942
$1s2p\ ^3P^o$	2.24544	492818	494273	493046
$1s2p\ ^1P^o$	2.28053	500520	501816	500645
$1s3s\ ^3S$	2.52080	553251	554761	553113
$1s3s\ ^1S$	2.53932	557316	558779	557223
$1s3p\ ^3P^o$	2.54217	559862	559501	557882
$1s3d\ ^3D$	2.55022	559708	561245	559464
$1s3d\ ^1D$	2.55036	559740	561276	559486
$1s3p\ ^1P^o$	2.55287	560290	561749	560188
$1s4s\ ^3S$	2.63587	578507	579982	578329
$1s4s\ ^1S$	2.64309	580092	581590	579932
$1s4p\ ^3P^o$	2.64436	580369	581897	580194
$1s4d\ ^3D$	2.64754	581069	582612	580821
$1s4d\ ^1D$	2.64763	581087	582631	580839
$1s4f\ ^3F^o$	2.64764	581089.7	582644	580839
$1s4f\ ^1F^o$	2.64764	581089.8	582645	580839
$1s4p\ ^1P^o$	2.64871	581325	582832	581139
$2s^2\ ^1S$	5.36391	146.0	146.2[c]	
$2s2p\ ^3P^o$	5.39476	146.8	147.0[c]	
$2p^2\ ^3P$	5.47781	149.1		
$2p^2\ ^1D$	5.50623	149.8	149.4[c]	
$2s2p\ ^1P^o$	5.51730	150.1	150.3[d]	
$2p^2\ ^1S$	5.65176	153.8		
$2s3s\ ^3S$	5.83412	158.7		
$2p3s/2s3p\ ^1P^o$	5.84384	159.0		
$2s3s\ ^1S$	5.85657	159.4		
$2s3p/2p3s\ ^3P^o$	5.86729	159.6		

[a] cm^{-1} for singly excited states; eV for doubly excited states.
[b] Singly excited states.
[c] Wuillemier [18].
[d] Candl and Kennedy [19].

ground-state energy that is too high by this amount. We note that, with the exception of $2p^2\ ^1D$, this constant difference also occurs for those doubly excited states where comparison can be made. We have also checked the values of the oscillator strengths of transitions between the target states. The results are too extensive to present here, but we note that (a) there is good agreement between length and velocity forms (better even than in paper I), (b) there is good agreement with the highly accurate calculation of Schiff *et al.* [20]. We therefore conclude that the target state wave functions are of sufficiently good quality for use in the present collisional calculations.

III. PHOTOIONIZATION CROSS SECTIONS

Partial photoionization cross sections were calculated for the following process:

$$1s^2 2s\ ^2S + h\nu \rightarrow 2lnl'n''l''\ \ ^2P^o \rightarrow [1snl + e(kl')]\ ^2P^o \rightarrow [2lnl' + e(kl'')]\ ^2P^o, \tag{6}$$

where the final Li^+ states are either singly excited ($1snl$) or doubly excited ($2lnl'$). The initial bound states and final continuum states of the $(N+1)$-electron system are calculated with the same parameters as were used in paper I: R-matrix radius $a=30.2a_0$; there are $N^{\mathrm{Cont}}=38$ continuum basis functions for each orbital angular momentum in the range $0 \leqslant l \leqslant 4$. In Table IV we give, for each of the two $SL\pi$ states of the $(N+1)$-electron system, the number N^B of bound configurations built from the orbitals involved in the target states, together with the number N^{Ch} of channels in Eq. (1) where $N^F = N^{\mathrm{Ch}} N^{\mathrm{Cont}}$.

TABLE IV. $Li^+ + e^-$: Number of channels N^{Ch} and corresponding bound terms N^B for each $SL\pi$ state.

State	N^{Ch}	N^B
$^2S^e$	28	486
$^2P^o$	44	921

TABLE V. Energies (in eV) of the $2l2l'$ ionization thresholds above the atomic lithium ground state.

Threshold	$2s^2\ ^1S$	$2s2p\ ^3P$	$2p^2\ ^3P$	$2p^2\ ^1D$	$2s2p\ ^1P$	$2p^2\ ^1S$	$2s3s\ ^3S$	$2s3s\ ^1S$
Energy (eV)	151.343	152.182	154.441	155.215	155.520	159.175	164.137	164.748

A first critical test of this mathematical model is provided by a comparison of the calculated energies and oscillator strengths of the combined $Li^+ + e^-$ system with the values obtained in other work. A particular difficulty in the present calculation, compared with the calculations of paper I, occurs because of the gap in energy between the target states $1s4p\ ^1P^o$ and $2s^2\ ^1S$. In this energy gap ($\sim$74 eV) there are embedded target states associated with correlation-type configurations $1s5l$. These are not real spectroscopic states and must be excluded from the first summation in Eq. (1). The exclusion procedure had to be taken into account carefully in the *R*-matrix code for the present study. In addition, a consistent CI selection, as defined in Vo Ky *et al.* [21], retains only those $(N+1)$-electron correlation functions Φ_j [second summation in Eq. (1)], which have corresponding ''parent'' terms in the *N*-electron system.

The present calculated effective quantum numbers for the two series $1s^2ns\ ^2S$ and $1s^2np\ ^2P^o$ are slightly improved over the values obtained in paper I. The length and velocity forms of the oscillator strengths of ^2S-$^2P^o$ transitions agree to within a few percent of each other and with established tabulated data [22].

For photon incident energies in the 140–167-eV range, the photoionization process gives rise to different Rydberg series of resonant states $2l2l'nl''\ ^2P^o$: $(2s^2\ ^1S)np$, $(2s2p\ ^3P)ns,nd$, $(2p^2\ ^3P)np$, $(2p^2\ ^1D)np$, $(2s2p\ ^1P)ns,nd$ and $(2p^2\ ^1S)np$ for photon energies lower than 160 eV and some $2l3l'nl''\ ^2P^o$ for photon energies between 160 and 167 eV. With our calculated energy for the ground state $1s^22s\ ^2S$, the corresponding theoretical ionization threshold energies are given in Table V.

Partial photoionization cross sections were calculated from the ground state of Li, leaving the Li^+ ion in any one of the 29 states listed in Table III. We considered the energy

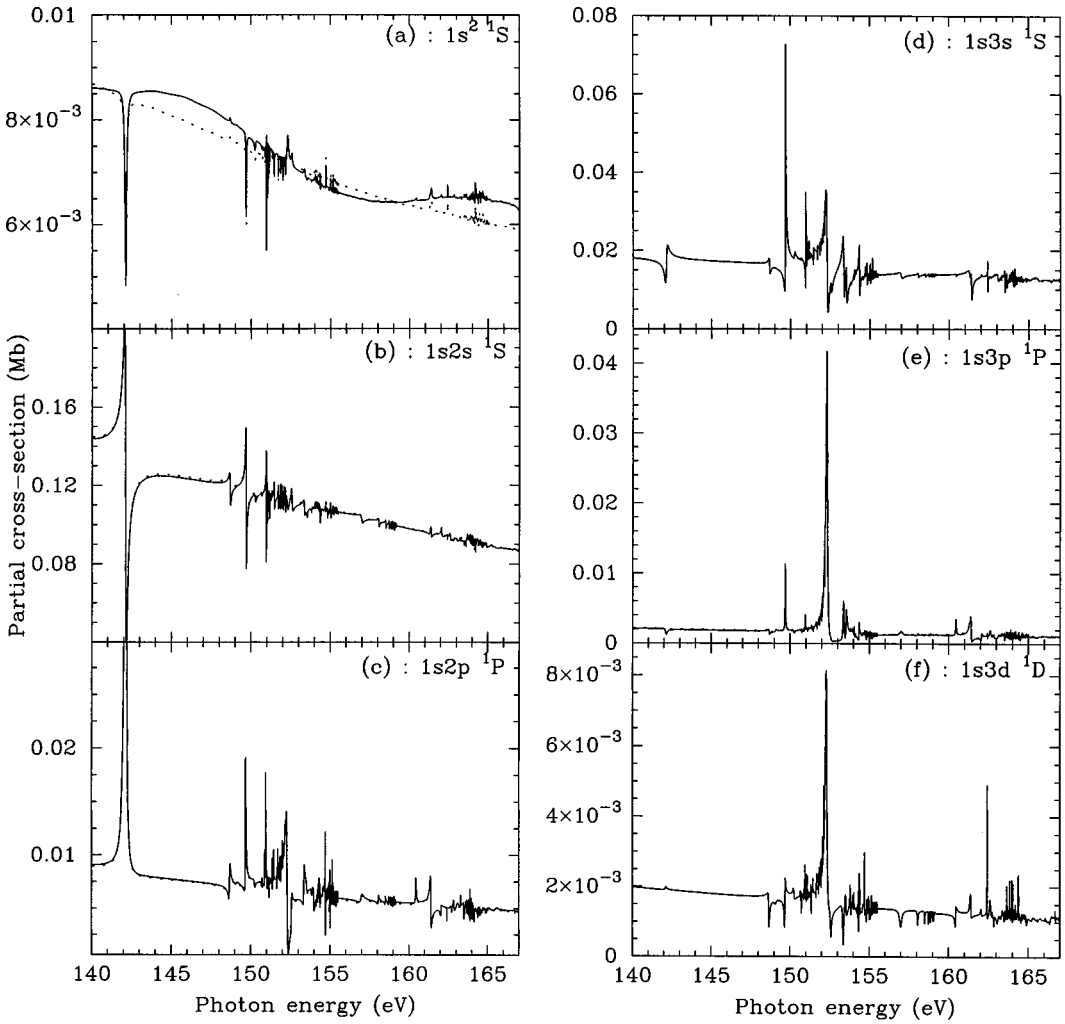

FIG. 1. Theoretical partial cross section (in megabarns) for photoionization of $1s^22s\ ^2S$ lithium ground state leaving the Li^+ ion in different final ionic state $1snl\ ^1L$ at incident photon energies between 140 and 167 eV. (a) $1s^2\ ^1S$; (b) $1s2s\ ^1S$; (c) $1s2p\ ^1P^o$; (d) $1s3s\ ^1S$; (e) $1s3p\ ^1P^o$; (f) $1s3d\ ^1D$. Full line, length form; dotted line, velocity form.

range of 140–167 eV, and used an energy mesh of 5×10^{-4} Ry (0.0068 eV). Typical results are shown in Figs. 1(a)–1(f) in which the Li^+ ion is left in the $1snl\ ^1L$ states for $n=1,2,3$. (A qualitatively similar set of results is obtained for final Li^+ states of the form $1snl\ ^3L$; the results are larger by about a factor 3, because of the multiplicity.) Except for the $1s^2\ ^1S$ final state, there is better than 2% agreement between length and velocity forms, thus providing further confirmation of the adequacy of the present mathematical model. From these calculations, we have estimated the positions of the different ionization thresholds, whose values are presented in Table V. (Other partial cross-section data are available on request).

IV. COMPARISON WITH EXPERIMENTAL MEASUREMENTS

In recent years, attention has been focused on photon-Li atom impact experiments resulting in the population of highly correlated hollow Li atomic states where all three excited electrons reside outside the *K* shell. Different experimental techniques were used in order to obtain either photoabsorption spectra [1], photoion spectra [2,4], or photoelectron spectra [5–8]. In the two first cases, experimental measurements give the total photoionization cross section. In photoelectron spectroscopy, partial photoionization cross sections can also be measured. This permits a more detailed comparison between experimental data and theoretical results.

A. Results in the vicinity of the lowest Li hollow state

The lowest triply excited resonance—$2s^2 2p\ ^2P^o$—around 142.2 eV has been extensively studied in the last few years. Computed and measured Fano parameters for this resonance profile have already been published [1,4,6]. In particular, the parameter values obtained in the present *R*-matrix calculations and published by Diehl *et al.* [6] were in good agreement with data obtained from high-resolution experiments.

Partial photoionization cross sections were measured using photoelectron spectroscopy by Journel *et al.* [5]. Their results concern the Li^+ ion being left in any of the $1s2l$ states, and some comparisons were made with *R*-matrix calculations, convoluted with the instrumental resolution. More extensive results are given in the present paper. In Figs. 2(a)–2(d) we compare the calculated partial photoionization cross sections leaving the ion respectively in the states $1s2s\ ^3S$, $1s2s\ ^1S$, $1s2p\ ^3P^o$, $1s2p\ ^1P^o$ with the corresponding experimental cross sections obtained by Wuilleumier's group [5,23] and we add, in the insets, some unpublished comparisons with *R*-matrix calculations convoluted with the instrumental resolution. We note that the agreement between length and velocity results is excellent. For absolute cross sections such as these, the main limitation is the uncertain accuracy of the experimental cross sections: they are measured only to about 25% accuracy [24]. This uncertainty must be added to the error bars inherent to the measurement process. In Figs. 2(a)–2(d), we show this additional uncertainty only for the lowest-energy experimental point. Agreement between theory and experiment is quite good, since there is no normalization of the experimental results to any theoretical parameter.

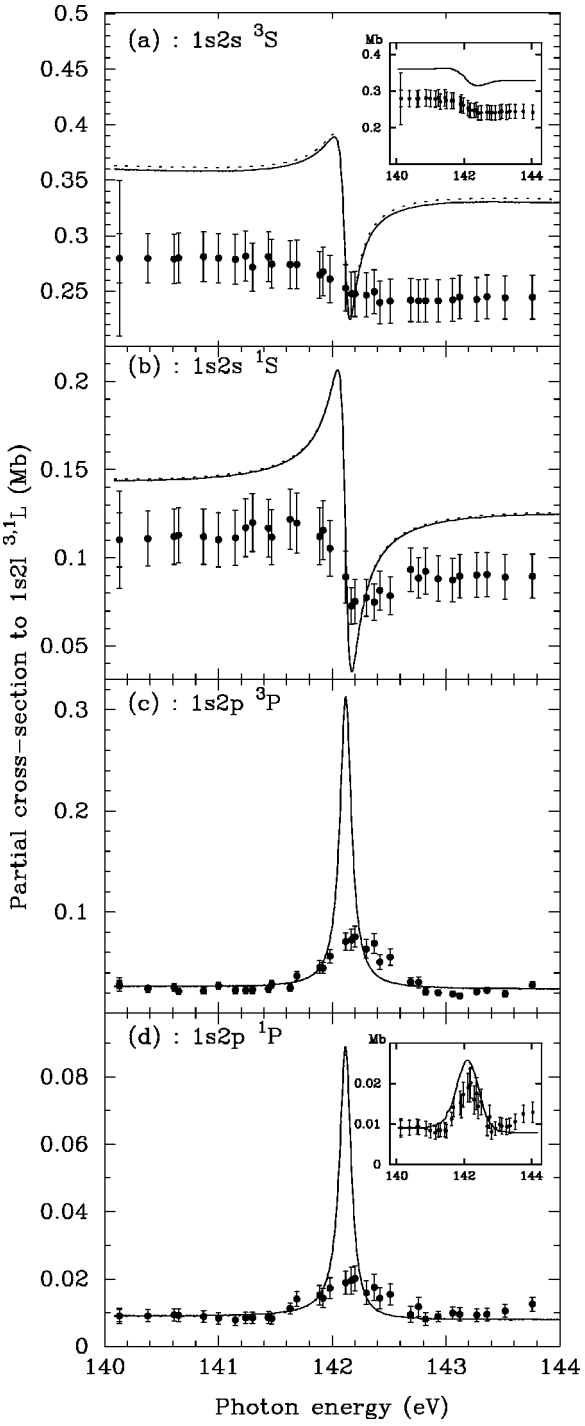

FIG. 2. Photoionization partial cross section (in megabarns) of lithium atoms to the different final ionic states $1s2l\ ^{1,3}L$ over the photon energy region of the first excited resonance at 142.2 eV. (a) $1s2s\ ^3S$; (b) $1s2s\ ^1S$; (c) $1s2p\ ^3P^o$; (d) $1s2p\ ^1P^o$. Full line, length form; dotted line, velocity form. (●) Experimental measurements from Wuilleumier's group [5,21]. In the insets, the *ab initio* *R*-matrix calculations are convoluted with the instrumental resolution.

B. Total photoionization cross sections

Photoion yield spectra giving total photoionization cross sections of hollow Li were measured with good resolution

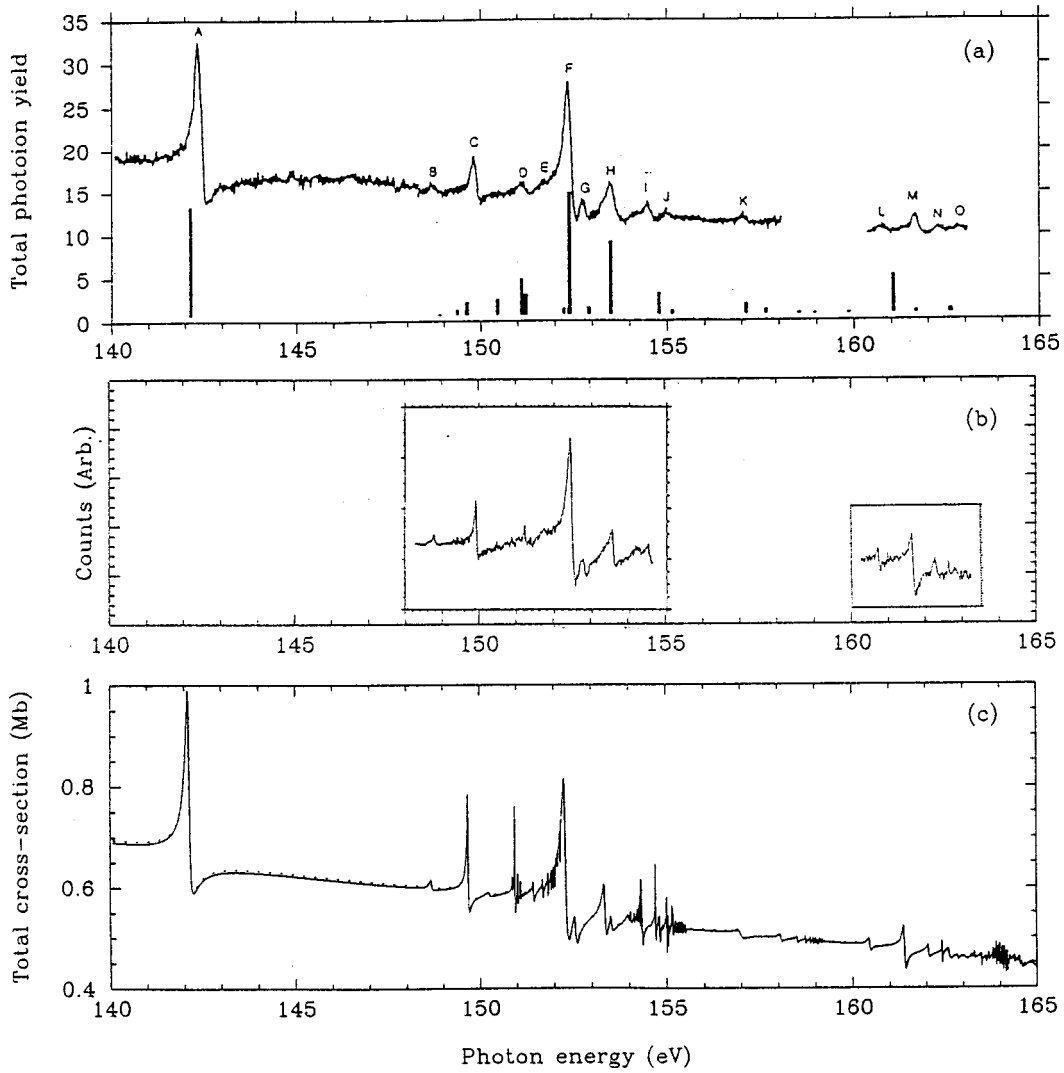

FIG. 3. Total photoionization cross section of lithium atoms in the 140–165-eV incident photon energy range. (a) Photoion measurements [4]; (b) photoion measurements [2]; (c) present theoretical results: full line, length form; dotted line, velocity form.

(0.03 eV for Azuma *et al.* [4], 0.02 eV for Kiernan *et al.* [2]) and for photon energies up to 165 eV. In this photon energy range, resonances for energies lower than 160 eV are due to $2l2l'nl''\ ^2P^o$ autoionizing states whereas for energies higher than 160 eV, resonances are due to $2l3l'nl''\ ^2P^o$ autoionizing states. Figure 3 compares the present *ab initio* calculations [Fig. 3(c)] with these two experimental results: Fig. 3(a) (Azuma *et al.* [4]) and Fig. 3(b) (Kiernan *et al.* [2]). Agreement is quite good throughout this energy range if we shift the present results by about 0.2 eV. This shift is needed because, as we noted earlier, the Li^+ ground-state energy is too high by approximately this amount relative to all the other target states. The very narrow but intense theoretical resonances (for example, around 151 eV) have a measured profile considerably enlarged by the instrumental resolution and this explains the relative importance of some experimental line intensities compared with the theoretical ones. Assignments of the observed features will be discussed in Sec. VII.

C. Partial photoionization cross sections

The earlier photoion experiments demonstrated a rich spectrum of multiply excited states in the 140–165-eV energy range. Because of cancellation effects, particular resonances may sometimes be very weak in such experiments but be large if observed using photoelectron spectroscopy in a specific decay channel. Using this technique, Wuilleumier's group measured photoionization cross sections at the Advanced Light Source in Berkeley [6–8]. Their experimental measurements were concerned with partial photoionization cross sections leaving the Li^+ ion not only in a $1snl\ ^{1,3}L$ $(n=2,3,4)$ state but also in some $2l2l'\ ^{1,3}L$ states. Our mathematical model includes the calculation of the partial photoionization cross sections leaving the Li^+ ion in any $2l2l'\ ^{1,3}L$ state. Figure 4 shows the theoretical variation of these partial photoionization cross sections for incident photon energies from each corresponding threshold energy of Li^+, as defined in Table V, up to 167 eV. All the already published detailed comparisons between experimental measurements and calculated partial cross sections for photoionization of $1s^22s\ ^2S$ Li atoms either into a $1snl\ ^{1,3}L$ final ionic state [5–7] or to a $2l2l'\ ^{1,3}L$ final ionic state [7,8] show a good agreement demonstrating the quality of the present mathematical model for incident photon energies up to 167 eV.

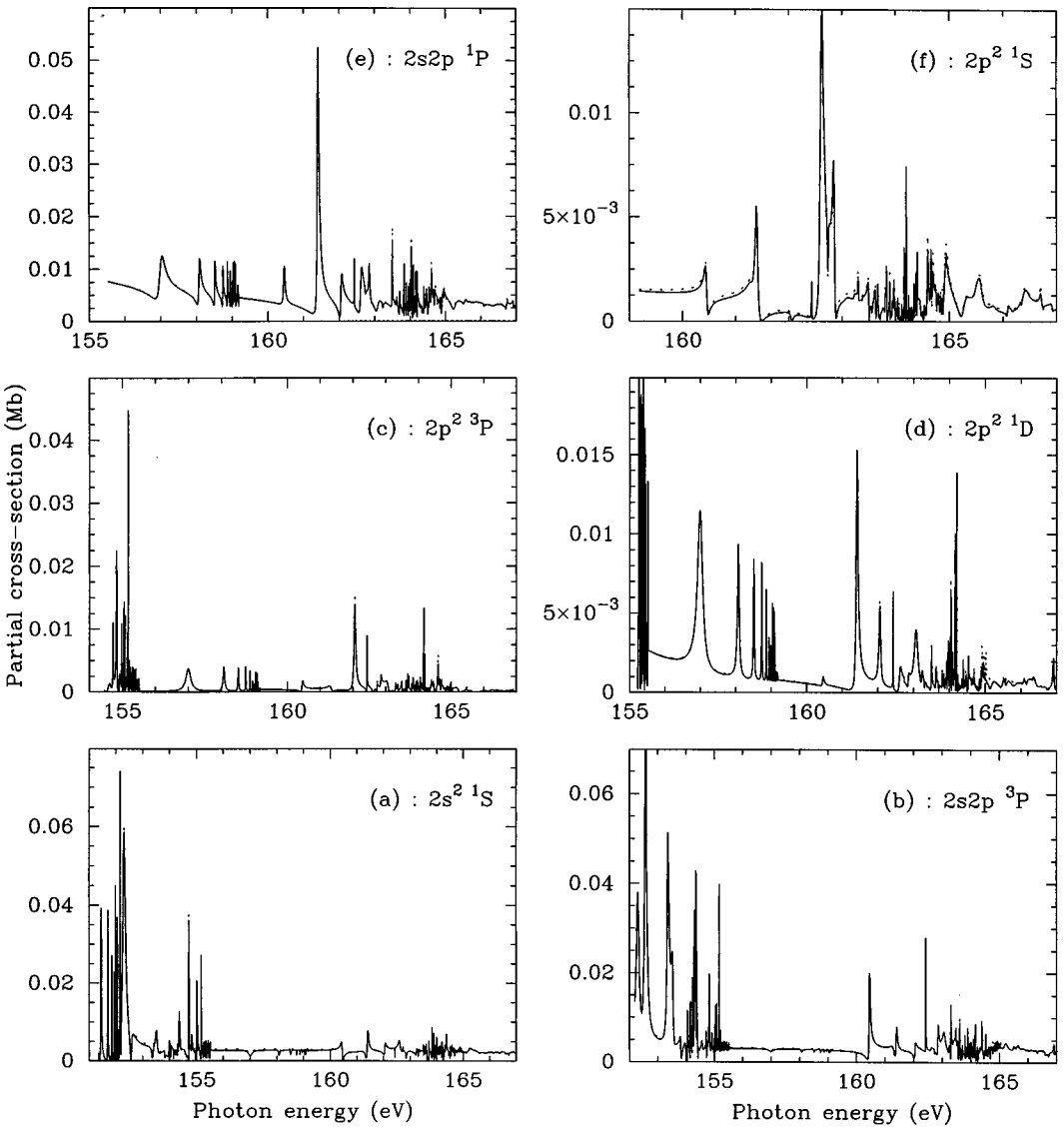

FIG. 4. Theoretical partial cross section (in megabarns) for photoionization of $1s^22s\ ^2S$ lithium ground state leaving the Li^+ ion in different final ionic state $2l2l'\ ^{1,3}L$ at incident photon energies from each corresponding threshold up to 167 eV. (a) $2s^2\ ^1S$; (b) $2s2p\ ^3P$; (c) $2p^2\ ^3P$; (d) $2p^2\ ^1D$; (e) $2s2p\ ^1P$; (f) $2p^2\ ^1S$. Full line, length form; dotted line, velocity form.

V. PARTIAL PHOTOIONIZATION CROSS-SECTION BRANCHING RATIOS

While experimental determination of the absolute values of partial photoionization cross sections may be a difficult procedure, it is nonetheless possible to measure accurately *relative* intensities of different photoionization processes. From the present calculations, it is simple to determine branching ratios of theoretical partial photoionization cross sections or indeed the sum of any number of them. This provides a useful further test of our model. For hollow Li, branching ratios have been measured at the LSAI in Orsay for photon energies in the energy range 140–144 eV, though only between partial cross sections in which the Li^+ ion is left in a $1s2l$ state. Figures 5(a)–5(c) compare respectively the theoretical branching ratio $\sigma(1s^22s\ ^2S \rightarrow 1s2s\ ^1S)/\sigma(1s^22s\ ^2S \rightarrow 1s2s\ ^3S)$, $\sigma(1s^22s\ ^2S \rightarrow 1s2p\ ^3P^o)/\sigma(1s^22s\ ^2S \rightarrow 1s2s\ ^3S)$, and $\sigma(1s^22s\ ^2S \rightarrow 1s2p\ ^1P^o)/\sigma(1s^22s\ ^2S \rightarrow 1s2s\ ^3S)$ with the experimental ratios. The average of the measured ratio outside the resonance zone around 142.2 eV is identical to the theoretical one and the error bar of 25% does not exist for these relative intensities. For each branching ratio, the experimental measurements [23] are compared with the results obtained from the *ab initio R*-matrix calculations in the main figures and, in the insets, with *R*-matrix calculations after convolution with the instrumental resolution. In comparison with Figs. 2(a)–2(d), which give absolute cross sections, agreement between theoretical and measured branching ratios is much improved. Moreover, the theoretical results obtained with the length and velocity formulations are essentially identical, confirming further the high quality of the calculations.

As an example of the branching ratio obtained in the whole energy range between 140 and 167 eV, Fig. 6 compares the sum of partial cross sections leaving Li^+ in a $1s3l$ final ionic state to the similar sum for a $1s2l$ final ionic state: $\Sigma_l\sigma(1s^22s\ ^2S \rightarrow 1s3l\ ^{1,3}L)/\Sigma_l\sigma(1s^22s\ ^2S \rightarrow 1s2l\ ^{1,3}L)$. Comparative experimental measurements do not exist. From this figure we also notice the rate to a final ionic state $1s3l$ is about 25% of the rate to $1s2l$ away from resonances.

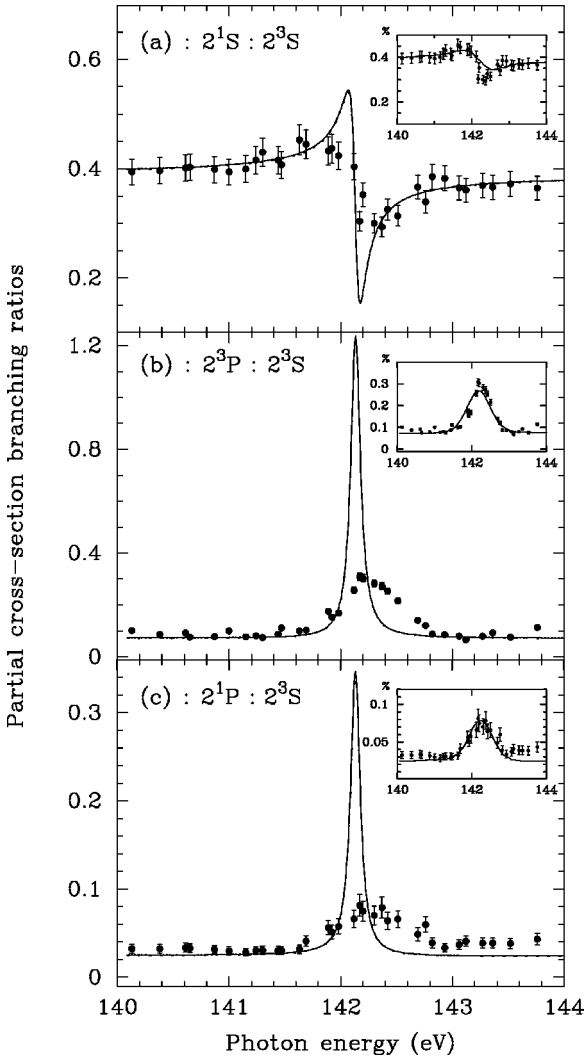

FIG. 5. Partial cross-section branching ratios over the photon energy region of the $2s^22p\ ^2P^o$ hollow Li state. (a) $\sigma(1s^22s\ ^2S \rightarrow 1s2s\ ^1S)/\sigma(1s^22s\ ^2S \rightarrow 1s2s\ ^3S)$; (b) $\sigma(1s^22s\ ^2S \rightarrow 1s2p\ ^3P^o)/\sigma(1s^22s\ ^2S \rightarrow 1s2s\ ^3S)$; (c) $\sigma(1s^22s\ ^2S \rightarrow 1s2p\ ^1P^o)/\sigma(1s^22s\ ^2S \rightarrow 1s2s\ ^3S)$. Present theoretical results: Full line where length form and velocity form are superimposed. (●) Experimental measurements from Wuilleumier's group [23]. In the insets, the *ab initio R*-matrix calculations are convoluted with the instrumental resolution.

VI. ASYMMETRY PARAMETER

The expression for the asymmetry parameter β, which relates the differential cross section $d\sigma(L_iS_i \rightarrow L_fS_f)/d\hat{k}_f$ to the integrated cross section σ, is given in paper I. Any asymmetry parameter can be obtained from our theoretical results, for any transition leaving the ion in any state given in Table III and these are available from authors. As no experimental measurement has been done for the β asymmetry parameter in this photon energy range, Figs. 7(a) and 7(b) show, as an example, the theoretical values obtained from the present calculations in the 140–154-eV photon energy range for the two conjugate shakeup satellites $1s2p\ ^3P^o$ and $1s2p\ ^1P^o$. Results are quite similar for the two transitions. We note that for the two main lines $1s2s\ ^3S$ and $1s2s\ ^1S$, $\beta=2$ as predicted by theory [25].

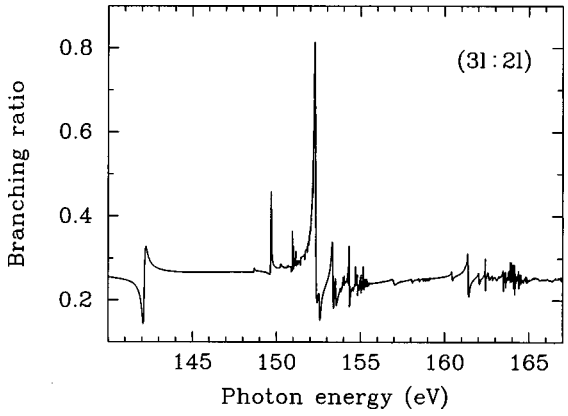

FIG. 6. Partial cross-section branching ratio $\Sigma_l\sigma(1s^22s\ ^2S \rightarrow 1s3l\ ^{1,3}L)/\Sigma_l\sigma(1s^22s\ ^2S \rightarrow 1s2l\ ^{1,3}L)$ in the 140–167-eV incident photon energy range.

VII. ASSIGNMENT OF THE RESONANCE ENERGY POSITIONS

Tentative assignments of the most prominent features in the 140–167-eV photon energy range were previously proposed by Azuma *et al.* [4], Kiernan *et al.* [2], Journel *et al.* [5] and Diehl *et al.* [6]. These assignments are based on theoretical calculations taking account of configuration interaction: multiconfiguration Dirac-Fock (MCDF) [4], configuration interaction Hartree-Fock (CIHF) [2], *R*-matrix [5,6]. However, the calculated energies were found to have a systematic shift to lower energies compared to experimental results. Thus, in Kiernan *et al.* [2], all computed energies have a 0.45-eV correction added to bring the computed (141.87

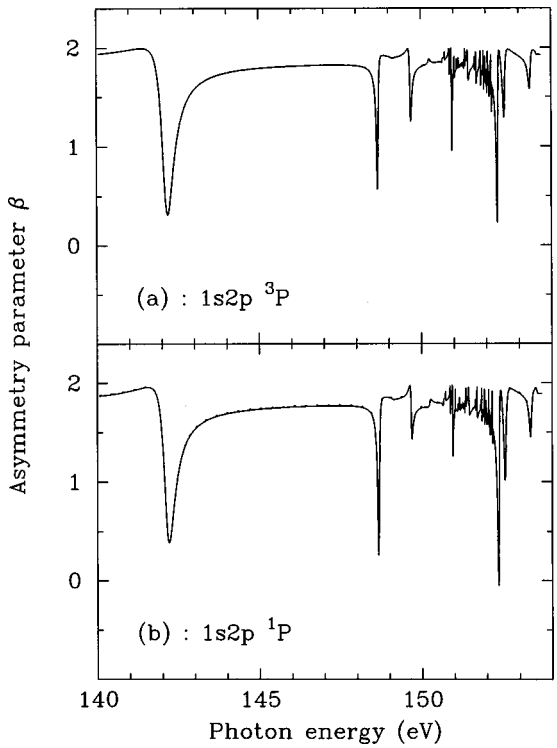

FIG. 7. Theoretical asymmetry parameter β for photoionization of $1s^22s\ ^2S$ lithium ground state leaving the Li^+ ion in the excited states: $1s2p\ ^3P^o$ (a) and $1s2p\ ^1P^o$ (b) in the 140–155-eV incident photon energy range.

TABLE VI. Assignment for $2l2l'n''l''\ ^2P^o$ resonances given for each series converging to the $2l2l'\ ^{2S+1}L$ ionization thresholds of Li.

	$2s^2(^1S)np$			$2s2p(^3P)ns$			$2s2p(^3P)nd$			$2p^2(^3P)np$		
n	Label	E (eV)	n^*	Label	E (eV)	n^*	Label	E (eV)	n^*	Label	E (eV)	n^*
2	p_2	142.12	1.22							p'_2	148.68	1.59
3	p_3	149.07	2.45	s_3	149.69	2.34	d_3	150.74	3.07	p'_3	152.57	2.70
4	p_4	150.24	3.51	s_4	150.95	3.32	d_4	151.36	4.07	p'_4	153.35	3.53
5	p_5	150.67	4.50	s_5	151.45	4.31	d_5	151.63	4.96	p'_5	153.81	4.64
6	p_6	150.88	5.42	s_6	151.71	5.37	d_6	151.82	6.13	p'_6	154.05	5.90
7	p_7	151.03	6.59	s_7	151.85	6.40	d_7	151.92	7.20	p'_7	154.15	6.84
8	p_8	151.11	7.64	s_8	151.93	7.35	d_8	151.98	8.20	p'_8	154.22	7.85
9	p_9	151.16	8.62	s_9	151.99	8.42	d_9	152.02	9.16	p'_9	154.27	8.92
10	p_{10}	151.20	9.65	s_{10}	152.03	9.46	d_{10}	152.05	10.15	p'_{10}	154.30	9.82
∞		151.343			152.182			152.182			154.441	
	$2p^2(^1D)np$			$2s2p(^1P)ns$			$2s2p(^1P)nd$			$2p^2(^1S)np$		
n	Label	E (eV)	n^*	Label	E (eV)	n^*	Label	E (eV)	n^*	Label	E (eV)	n^*
3	p''_3	153.52	2.83	s'_3	152.32	2.06	d'_3	153.35	2.50	p'''_3	156.97	2.48
4	p''_4	153.97	3.30	s'_4	154.05	3.04	d'_4	154.34	3.40	p'''_4	158.06	3.49
5	p''_5	154.56	4.56	s'_5	154.72	4.12	d'_5	154.83	4.44	p'''_5	158.51	4.52
6	p''_6	154.76	5.47	s'_6	155.02	5.22	d'_6	155.05	5.38	p'''_6	158.73	5.53
7	p''_7	154.90	6.57	s'_7	155.17	6.23	d'_7	155.20	6.52	p'''_7	158.86	6.57
8	p''_8	154.98	7.61	s'_8	155.26	7.23	d'_8	155.26	7.23	p'''_8	158.94	7.61
9	p''_9	155.03	8.57	s'_9	155.32	8.25	d'_9	155.32	8.25	p'''_9	158.99	8.57
10	p''_{10}	155.07	9.69	s'_{10}	155.36	9.22	d'_{10}	155.36	9.22	p'''_{10}	159.03	9.69
∞		155.215			155.520			155.520			159.175	

eV) and measured (142.32 eV) energy of the lowest $2s^22p(^2P^o)$ resonance into coincidence whereas in our R-matrix calculations the computed energy ($E[2s^22p(^2P^o)] = 142.12$ eV) is 0.20 eV lower than experiment. The corresponding energy value from MCDF results [4] is 141.657 eV whereas the best calculated value compared with the experimental one is obtained from the saddle-point technique [12] ($E = 142.255$ eV).

Eleven new lithium $2l2l'nl''\ ^2P^o$ resonances were calculated by Chung and Gou [13], between 149 and 154 eV, using the saddle-point technique and their calculated positions agree quite well with the experiments but the suggested identifications are not always the same.

A unified theory mixing R-matrix with MQDT (multichannel quantum defect theory) was recently proposed by Li *et al.* [26,27] allowing a much clearer assignment for resonances to be made. Such a method which calculates the wave functions of the total $(Li^+ + e)$ system outside the R-matrix box gives, from phase shifts and mixing coefficients, the energy states of the bound $(Li^+ + e)$ system. This method had already been applied in paper I. It shows that the observed position of the different resonances is sometimes shifted when comparing with these theoretical ones when resonances are overlapping. Assignments for some of the present $2ln'l'n''l''\ ^2P^o$ resonances were given by Li *et al.* [26] in the 140–154 eV photon energy range. In these previous results, the $2p^3$ resonance is obtained at 150.98 eV whereas this same resonance is calculated at 148.729 eV from the saddle-point technique [12]. This assignment of Li *et al.* [26] is probably due to strong channel interactions. On the other hand, the calculated positions of Li *et al.* [26] are given relative to $2l2l'$ ionization threshold values of Li, which are not very accurately estimated.

A new determination of the resonance positions for each series converging to a $2l2l'$ threshold of Li is proposed in this paper. We use the quantum defect approximation [28] which, in the present case, can be written as

$$(n^*)^{-2} = E_{\text{thres}}(2l2l'\ ^{2S+1}L) - E[(2l2l'\ ^{2S+1}L)nl''\ ^2P^o], \tag{7}$$

where energies are given in Rydberg units, $n^* = n - \mu_n$ and μ_n is the quantum defect. The energy values $E[(2l2l'\ ^{2S+1}L)nl''\ ^2P^o]$ are determined by considering the detailed symmetric or Fano profile and the numerical calculations of partial photoionization cross sections, which allow us to specify unambiguously the position of the resonances. For example, from the partial cross sections leaving the Li^+ ion into the $1s^2\ ^1S$ or $1s2s\ ^3S$ states, the resonance position calculated at 148.68 eV can be attributed to $2p^3\ ^2P^o$ without ambiguity. Such a detailed method was not applied for the previously suggested assignments from the R-matrix calculations [5,6]. Table VI gives for each series the position of the resonances determined from this method. Figure 8 displays the total photoionization cross section and locates the position of most of the resonances determined in the 142–154 eV photon energy range. The $2s^23p\ ^2P^o$ resonance (quoted p_3) is not noticeable in the total cross section and it can be only weakly observed on partial cross sections. Table VII compares in this same energy range the different theoretical or experimental assignments quoted in the litera-

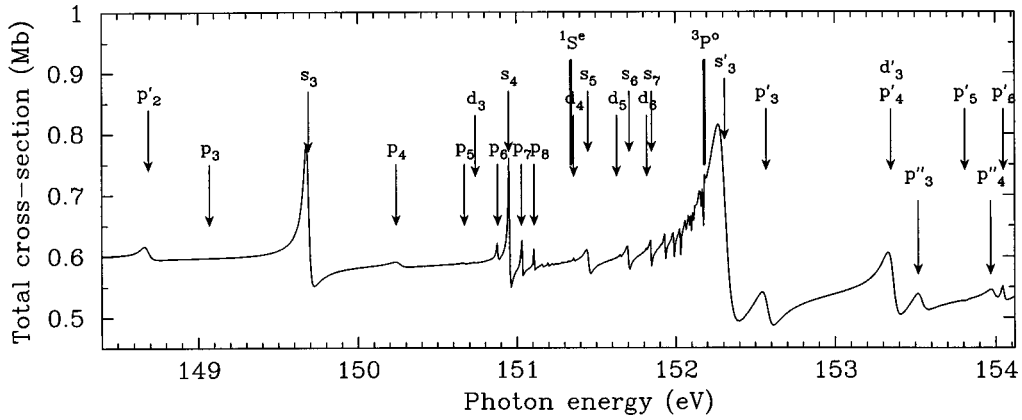

FIG. 8. Present assignment, labeled in Table VI, of the theoretical Rydberg series running up to the $2s^2\ ^1S$ threshold (151.343 eV), $2s2p\ ^3P$ threshold (151.182 eV), $2p^2\ ^3P$ threshold (155.441 eV) and $2p^2\ ^3P$ threshold (155.215 eV), in the 148–154 eV photon energy range, from present *ab initio* calculations.

ture. If we shift the energy values obtained by Li *et al.* [26] from the difference between the different threshold energies used, the two classes of results are quite similar except for four resonances: p_2', p_3, d_3, and p_6. As already mentioned, this can be due to important channel interactions which may modify the attributed assignments. The present determination of the resonance positions is with one exception in the same order as the energy calculations obtained from the saddle-point technique [12,13]. We note only an inversion between the two resonances labelled p_6 and s_4.

TABLE VII. Resonance energy positions $2l2l'n''l''\ ^2P^o$ listed in sequential form over the region of the first $2l2l'$ thresholds. Energies quoted from the literature have been positioned according to their spectral assignment. All mentioned theoretical calculations are *ab initio* without any shift.

Label	State	This work	Calc. [24] *R*-matrix+MQDT	Calc. [12,13] Saddle-point	Calc. [5,6] *R*-matrix	Calc. [4] CIHF	Calc. [2,3] MCDF	Expt. [6]	Expt. [4]	Expt. [2]
p_2	$2s^2(^1S)2p$	142.12	142.12	142.255	142.12	141.87	141.657	142.28	142.33	142.35
p_2'	$2p^3$	148.68	150.98	148.729	149.01	148.48	148.439		148.77	148.7
p_3	$2s^2(^1S)3p$	149.07	148.68	149.241		148.88				
s_3	$2s2p(^3P)3s$	149.69	149.61	149.846	149.70	149.38	150.008	149.98	149.91	149.79
p_4	$2s^2(^1S)4p$	150.24	150.19	150.480						
p_5	$2s^2(^1S)5p$	150.67	150.59	150.917						
d_3	$2s2p(^3P)3d$	150.74	150.88	150.947						
p_6	$2s^2(^1S)6p$	150.88	150.82	151.203						
s_4	$2s2p(^3P)4s$	150.95	151.03	151.119	150.97	150.88	150.665	151.25	151.20	151.10
p_7	$2s^2(^1S)7p$	151.03	150.97	151.349						
p_8	$2s^2(^1S)8p$	151.11	151.08							
	$2s^2(^1S)$ thres.	151.343	151.29		151.29					
d_4	$2s2p(^3P)4d$	151.36	151.30			151.14				
s_5	$2s2p(^3P)5s$	151.45	151.33							
d_5	$2s2p(^3P)5d$	151.63	151.58							
s_6	$2s2p(^3P)6s$	151.71	151.63							
d_6	$2s2p(^3P)6d$	151.82	151.74							
s_7	$2s2p(^3P)7s$	151.85	151.78							
d_7	$2s2p(^3P)7d$	151.92	151.85							
	$2s2p(^3P)$ thres.	152.182	152.13		152.13					
s_3'	$2s2p(^1P)3s$	152.32		152.453	152.48	152.37	151.955	152.90	152.75	152.32
p_3'	$2p^2(^3P)3p$	152.57	152.51	152.742	152.41	152.15	152.470	152.51	152.46	152.72
p_4'	$2p^2(^3P)4p$	153.35	153.29	153.572	153.48	153.13	153.042	153.66	153.54	153.43
p_3''	$2p^2(^1D)3p$	153.52	153.46							
p_5'	$2p^2(^3P)5p$	153.81	153.75							
p_4''	$2p^2(^1D)4p$	153.92	153.97							
p_6'	$2p^2(^3P)6p$	154.05	153.98							
	$2p^2(^3P)$ thres.	154.441	154.39		154.39					

VIII. CONCLUSION

The present *R*-matrix calculation includes photoionization from the ground state $1s^2 2s\ ^2S$ of neutral lithium for incident photon energies between 140 and 167 eV. This energy range allows us to account for resonances due to excited states corresponding to $2ln'l'n''l''$ configurations for $n'=2$ and 3. In the *R*-matrix code, the CC expansion of the Li^+ target is represented by 29 states and the CI expansion includes up to 369 basic configurations. In order to overcome the major difficulty due to the gap in energy between the target states $1s4p\ ^1P^o$ and $2s^2\ ^1S$, we had to exclude some nonphysical target pseudostates embedded in this energy gap. The high quality of the target wave functions as well as bound and continuum ones for the $Li^+ + e$ system is demonstrated by comparing calculated energies with experimental ones, and oscillator strengths with other sophisticated theoretical calculations. This quality in the results implies an extensive and correctly balanced configuration expansion for the target and for the $(N+1)$-electron states.

Partial photoionization cross sections are shown in some detail. They are the first theoretical results obtained in this energy range and they reproduce in the whole energy range between 140 and 165 eV, with a very good agreement, the most recent experimental ones observed by Wuilleumier's group [6–8].

Some branching ratios between partial cross sections and asymmetry parameters are also given and compared when possible with experimental ones. Other theoretical results for transitions to any state given in Table III are available on request.

Finally, an assignment is given for all the important resonances calculated in the 140–160-eV photon energy range, which converge to the $2l2l'\ ^{2S+1}L$ ionization thresholds of atomic lithium. These assignments allow us to confirm some identifications already proposed from other theoretical or experimental results in the 140–154-eV photon energy range.

ACKNOWLEDGMENTS

The calculations were carried out partly on the CRAY YMP/2E computer [at the IMT Marseille (France) supported by the Conseil Régional Provence-Alpes-Côte d'Azur] and partly on the CRAY C98 (IDRIS-France, Project No. 940052). We thank F. J. Wuilleumier's group for communicating unpublished experimental results. One of us (A.H.) acknowledges partial funding from the EC HCM Network, Contract No. CHRX-CT93-0361

[1] L. M. Kiernan, E. T. Kennedy, J.-P. Mosnier, J. T. Costello, and B. F. Sonntag, Phys. Rev. Lett. **72**, 2359 (1994).
[2] L. M. Kiernan, M.-K. Lee, B. F. Sonntag, P. Sladeczek, P. Zimmermann, E. T. Kennedy, J.-P. Mosnier, and J. P. Costello, J. Phys. B **28**, L161 (1995).
[3] R. D. Cowan, *The Theory of Atomic Structure and Spectra* (University of California Press, Berkeley, 1981).
[4] Y. Azuma, S. Hasegawa, F. Koike, G. Kutluk, T. Nagata, E. Shigemasa, A. Yagishita, and I. A. Sellin, Phys. Rev. Lett. **74**, 3768 (1995).
[5] L. Journel, D. Cubaynes, J.-M. Bizau, S. Al Moussalami, B. Rouvellou, F. J. Wuillemier, L. Vo Ky, P. Faucher, and A. Hibbert, Phys. Rev. Lett. **76**, 30 (1996).
[6] S. Diehl, D. Cubaynes, J.-M. Bizau, L. Journel, B. Rouvellou, S. Al Moussalami, F. J. Wuillemier, E. T. Kennedy, N. Berrah, C. Blancard, T. J. Morgan, J. Bozek, A. S. Schlachter, L. Vo Ky, P. Faucher, and A. Hibbert, Phys. Rev. Lett. **76**, 3915 (1996).
[7] S. Diehl, D. Cubaynes, F. J. Wuillemier, J.-M. Bizau, L. Journel, E. T. Kennedy, C. Blancard, L. Vo Ky, P. Faucher, A. Hibbert, N. Berrah, T. J. Morgan, J. Bozek, and A. S. Schlachter, Phys. Rev. Lett. **79**, 1241 (1997).
[8] S. Diehl, D. Cubaynes, E. T. Kennedy, F. J. Wuillemier, J.-M. Bizau, L. Journel, L. Vo Ky, P. Faucher, A. Hibbert, C. Blancard, N. Berrah, T. J. Morgan, J. Bozek, and A. S. Schlachter, J. Phys. B **30**, L595 (1997).
[9] U. I. Safronova and V. S. Senashenko, J. Phys. B **11**, 2623 (1978).
[10] R. L. Simons, H. P. Kelly, and R. Bruch, Phys. Rev. A **19**, 682 (1979).
[11] N. A. Piangos and C. A. Nicolaides, Phys. Rev. A **48**, 4142 (1993).
[12] K. T. Chung and B. C. Gou, Phys. Rev. A **52**, 3669 (1995).
[13] K. T. Chung and B. C. Gou, Phys. Rev. A **53**, 2189 (1996).
[14] L. Vo Ky, P. Faucher, A. Hibbert, J.-M. Li, Y.-Z. Qu, J. Yan, J. C. Chang, and F. Bely-Dubau, Phys. Rev. A **57**, 1045 (1998).
[15] J. F. Perkins, J. Chem. Phys. **42**, 3927 (1965).
[16] J. F. Perkins, Phys. Rev. **178**, 89 (1969).
[17] A. Hibbert, Comput. Phys. Commun. **9**, 141 (1975).
[18] F. J. Wuilleumier (private communication).
[19] P. K. Candl and E. T. Kennedy, Phys. Rev. Lett. **38**, 1068 (1977).
[20] B. Schiff, C. L. Pekeris, and Y. Accad, Phys. Rev. A **4**, 885 (1971).
[21] L. Vo Ky, H. E. Saraph, W. Eissner, Z. W. Liu, and H. P. Kelly, Phys. Rev. A **46**, 3945 (1992).
[22] W. L. Wiese, M. W. Smith, and B. M. Glennon, *Atomic Transitions Probabilities* (National Bureau of Standards, Washington, DC, 1966), Vol 1.
[23] F. J. Wuilleumier, D. Cubaynes, S. Diehl, Al Moussalami, L. Journel, and B. Rouvellou (private communication).
[24] G. Mehlman, J. W. Cooper, and E. B. Saloman, Phys. Rev. A **25**, 2113 (1982).
[25] D. Dill, A. F. Starace, and S. T. Manson, Phys. Rev. A **11**, 1596 (1975).
[26] J.-M. Li, L. Vo Ky, J. Yan, and Y.-Z. Qu, Chin. Phys. Lett. **13**, 902 (1996).
[27] J.-M. Li, L. Vo Ky, Y.-Z. Qu, J. Yan, P.-H. Zhang, H.-L. Zhou, and P. Faucher, Phys. Rev. A **55**, 3239 (1997).
[28] M. J. Seaton, Rep. Prog. Phys. **46**, 167 (1983).